Proc. Natl. Acad. Sci. USA
Vol. 90, pp. 3098–3102, April 1993
Neurobiology

Noninvasive somatosensory homunculus mapping in humans by using a large-array biomagnetometer

T. T. YANG*†‡, C. C. GALLEN*, B. J. SCHWARTZ*§, AND F. E. BLOOM*

*Department of Neuropharmacology, The Scripps Research Institute, La Jolla, CA 92037; †Department of Molecular Pathology, University of California at San Diego, La Jolla, CA 92093; and §Biomagnetic Technologies, Inc., San Diego, CA 92121

Contributed by F. E. Bloom, December 24, 1992

ABSTRACT **To validate the feasibility of precise noninvasive functional mapping in humans, a large-array biomagnetometer was used to map the somatosensory cortical locations corresponding to numerous distinct tactile sites on the fingers, hand, arm, and face in different subjects. Source localizations were calculated by using a single equivalent current dipole (ECD) model. Dipole localizations were transposed upon the corresponding subject's magnetic resonance image (MRI) to resolve the anatomic locus of the individual dipoles within a given subject. Biomagnetic measurements demonstrated that (*i*) there were distinct separations between the ECD locations representing discrete sites on the face and hand; (*ii*) the ECD localizations from facial sites clustered in a region inferior to ECD localizations from hand and digit sites; and (*iii*) there was clear spatial resolution of ECD locations representing closely spaced tactile sites on the hand and face. The ability of magnetoencephalography (MEG) to provide high-resolution spatial maps of the somatosensory system noninvasively in humans should make MEG a useful tool to define the normal or pathological organization of the human somatosensory system and should provide an approach to the rapid detection of neuroplasticity.**

Functional mapping of the human somatosensory system has commonly used invasive surgical techniques which involve electrical stimulation of the brain (1), direct recordings of evoked potentials and electrical stimulation (2), somatosensory evoked responses (SERs) recorded on electrocorticography (ECoG) (3), or cortical surface recordings of somatosensory evoked potentials (SEP) during surgery (4, 5). The invasiveness of these approaches has limited the number of patients which may be studied and the types of questions which may be addressed. However, a variety of neuroimaging tools have been developed which may noninvasively study human mental functions. The human somatosensory cortex has been partially mapped using positron emission tomography (PET) (6), electroencephalography (EEG) (7–9), and magnetoencephalography (MEG) (10–18).

MEG offers certain unique advantages for somatosensory system mapping. EEG measures are prone to nonfunctional variations such as skull inhomogeneities and cerebrospinal fluid. Both of these nonfunctional variations can affect conductivity, but they have relatively little effect on the magnetic fields (19). The propensity of MEG to detect a subset of sources oriented tangentially to a line radiating from head center to head surface, combined with the attenuation of distant magnetic sources, results in a simpler field pattern more amenable to modeling as a single equivalent current dipole (ECD). Such modeling has produced highly reliable and accurate source localizations (20). The estimation of the statistical reliability and neuroanatomical validity of neuromagnetic somatosensory source localizations, along with the quantification of the sources of variability using a single ECD model, has been carried out for repeated measures within one subject (21).

The publication costs of this article were defrayed in part by page charge payment. This article must therefore be hereby marked "*advertisement*" in accordance with 18 U.S.C. §1734 solely to indicate this fact.

METHODS

Somatosensory stimulus-evoked magnetic brain activity generated by the left and right cortex in two neurologically normal undergraduate male subjects was recorded inside of a magnetically shielded room by using a Magnes 37-channel biomagnetometer (Biomagnetic Technologies, San Diego). The neuromagnetic field pattern was recorded over a 144-mm-diameter circular area above the parietotemporal cortex. Intrinsic noise in each channel was <10 fT/Hz$^{1/2}$ in all but one channel.

The biomagnetometer was placed over the contralateral hemisphere relative to the side being stimulated. Subjects were instructed to hold extremely still, and to count silently the number of stimuli.

Tactile stimulators provided skin surface stimulation. The stimulators, which were circular rubber bladders of 1 cm diameter encased within a plastic outer shell, expanded with air during each time period corresponding to a single stimulus. During each expansion, the stimulator provided a light, superficial pressure stimulus to the skin surface. At each stimulation site, a series of 256, 512, or 1024 stimuli were delivered with a randomly jittered interstimulus interval of 450–550 msec. The 37 sensors were all sampled at a frequency of 861 Hz, and the signals were bandpassed at 0.1–95 Hz. The trials for each session were averaged together and then digitally filtered with a bandpass of 2.5–40.0 Hz. Each data epoch spanned 300 msec, centered at the time of stimulus onset.

The somatosensory component peaking in the 40- to 89-msec latency range was localized with the single ECD model. Within this time window, only those ECD fits with correlations of 0.98 or greater, confidence volumes of less than 1.0 cm^3, and root mean square (rms) signal-to-noise ratios of greater than two were accepted as reliable fits. A correlation of 0.979 was accepted for one site (RInfraOrb) on subject 2. This ECD fit met all of the other listed criteria. If there were multiple dipoles meeting all of the selection criteria for a given stimulus site, then the dipole chosen for the magnetic resonance image (MRI) overlay was the location having both the highest correlation and the smallest confidence volume.

Stimulation sites on the skin surface were determined by using specific measured distances from anatomical landmarks found on each subject (see Fig. 1). The stimulation sites along the lower jaw were determined by measuring the distance from the corner of the mandibular angle to the point

Abbreviations: MRI, magnetic resonance image; ECD, equivalent current dipole; MEG, magnetoencephalography; EEG, electroencephalography.

‡To whom reprint requests should be addressed at: Department of Neuropharmacology, The Scripps Research Institute, 10666 North Torrey Pines Road, BCR1, La Jolla, CA 92037.

located on the bottom of the chin. This total distance was then multiplied by the values ¼, ½, and ¾ to obtain the distance measured from the mandibular angle for the stimulation sites ¼ mandible–chin, ½ mandible–chin, and ¾ mandible–chin, respectively. The mandibular angle was palpated to determine the stimulation point for this site. A spot 1 cm lateral to the point located precisely at the bottom of the chin was used for the stimulation site submental vertex. The site located halfway between the submental vertex and the bottom edge of the lower lip was chosen as the mental protuberance. The site located midway between the two corners of one eye, and midway between the medial corner of the eye and lateral edge of the bottom of the nose, was selected to be infraorbital. The corner of the mouth site was found by moving 1 cm lateral to the edge of the mouth. The zygomatic prominence site was located by measuring 3 cm below the lateral corner of the eye and 5 cm lateral to the bottom edge of the nose. The cheek site was found at the point midway between the bottom lateral edge of the nose and the bottom edge of the earlobe. The midzygomatic point was placed at a point 2 cm lateral to the corner of the eye. The stimulation sites along the forearm were determined by measuring the distance from the wrist to the point located over the cubital fossa. This total distance was then multiplied by the values ¼, ½, and ¾ to obtain the distance measured from the wrist for the stimulation sites ¼ forearm, ½ forearm, and ¾ forearm, respectively. This procedure was done twice: once for the sites along the T1 dermatome, and once for the sites along the C6 dermatome on the forearm. Each dermatome refers to the area of skin innervated by a single dorsal root—i.e., T1 or C6. The sites for the anterior and posterior wrist were located midway between the lateral edges of the forearm.

Orthogonal coronal, sagittal, and axial MRIs were obtained by using a General Electric (GE) Signa 1.5-T system. The T1-weighted contrast between cortical gray matter and adjacent white matter was maximized through inversion recovery sequences for subject 1. A "spoiled GRASS" (gradient recalled acquisition of the steady-state) pulse sequence was used to obtain the MRI for subject 2. The nasion, Cz, and bilateral preauricular points were identified on MRIs with the aid of high-contrast cod liver oil capsules which were affixed to these points on the scalp for subject 1. For subject 2, the two fiduciary points inside of both ears were identified on MRIs through the use of specially designed ear plugs which fit snugly within each ear. Each 3-mm MRI overlay slice presented in this study contains only the ECD locations of those particular dipoles which were uniquely found in that given MRI section.

Details regarding instrumentation, data analysis, MRI overlays, and techniques used to obtain the data and results are described by Gallen *et al.* (21).

RESULTS

A total of 66 tactile sites, bilaterally (14 facial, 44 hand, and 8 arm loci) were stimulated on each subject (Fig. 1). MRI overlays using the calculated single ECDs showed clear spatial separation of closely located facial, hand, and arm tactile sites. On the right side of the face, ECD locations corresponding to closely spaced anatomical sites such as the upper lip, mental protuberance, and corner of the mouth mapped to distinctly separable, but adjacent locations on the MRI coronal section (Fig. 2). ECD locations corresponding to closely spaced anatomical sites along the bottom of the left jaw extending from the mandibular angle to the ¾ mandible–chin mapped to sites on the MRI sagittal section which extended in an anterior–posterior direction (Fig. 3). The ECD locations corresponding to sites on the left mandibular angle and extending progressively towards the bottom of the chin seemed to be arranged in accord with the following anatomic

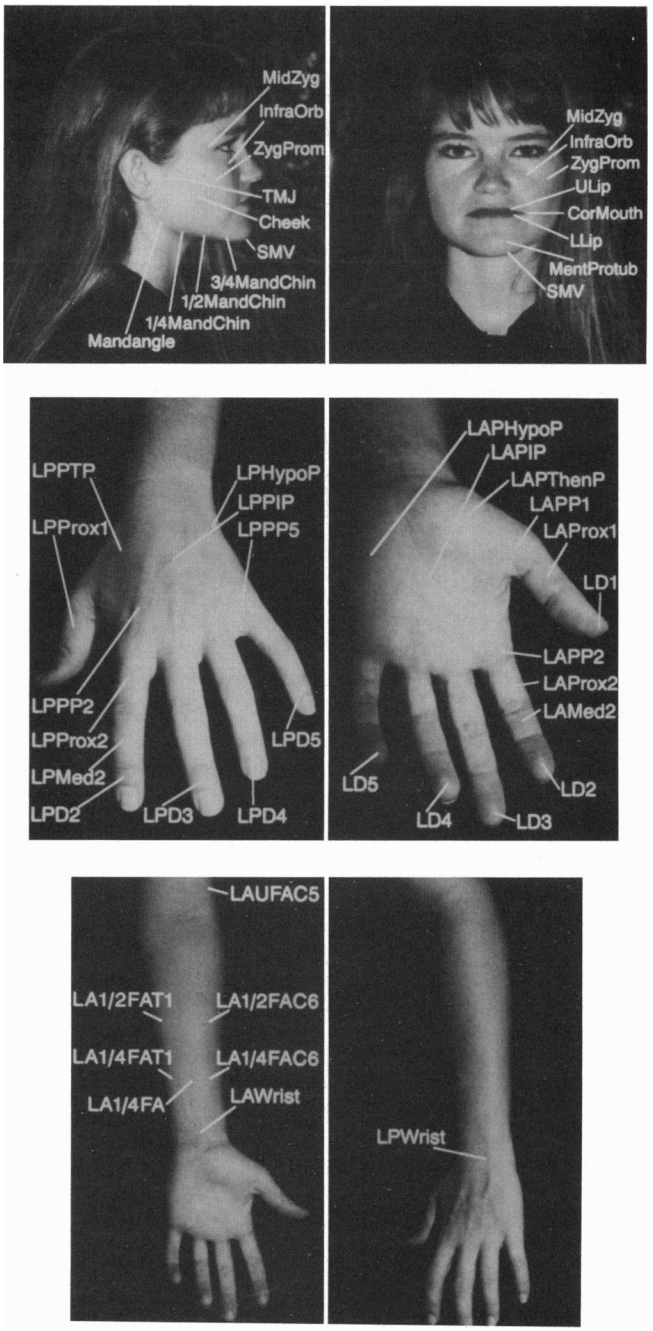

FIG. 1. (*Top*) Tactile stimulation sites on the right and left sides of the face. MidZyg, midzygomatic; InfraOrb, infraorbital; ZygProm, zygomatic prominence; TMJ, temporal mandibular joint; SMV, submental vertex; MandChin, mandible–chin; MandAngle, mandibular angle; ULip, upper lip; CorMouth, corner of mouth; LLip, lower lip; and MentProtub, mental protuberance. (*Middle*) Tactile stimulation sites on the posterior and anterior sides of the left hand. LP, left posterior; and LA, left anterior. PTP, palmar thenar pad; Prox1, proximal 1; PP2, palmar pad 2; Med2, medial 2; D2, digit 2; HypoP, hypothenar pad; PIP, palmar intermediate pad; PThenP, palmar thenar pad; and LD1, left (anterior) digit 1. (*Bottom*) Tactile stimulation sites on the anterior and posterior sides of the left arm. LA, left anterior; and LP, left posterior. FAT1, forearm T1 dermatome; FA, forearm; FAC6, forearm C6 dermatome; and UFAC5, upper arm C5 dermatome. In all figures, the prefix L indicates the left side of the body, and the prefix R indicates the right side of the body.

sequence: mandibular angle, ½ mandible–chin, ¾ mandible–chin. The ECD locations appeared to march along the sagittal MRI in the opposite anterior–posterior direction relative to

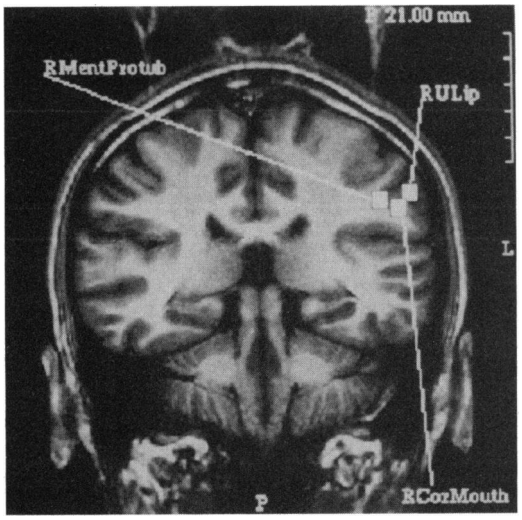

FIG. 2. Coronal section on subject 1 showing location of dipoles corresponding to tactile sites on the right side of the face. Each mark on the upper right vertical bar represents 1 cm. The letter L found in the middle of the right side of Figs. 2 and 4–7 indicates the left hemisphere of the brain. The letter and number found at the top right corner of all the figures indicates the position of the MRI slice in a defined, positive-number coordinate system: L, left, and R, right, with the nasion defined as 0.00 mm and A, anterior, and P, posterior, with the line connecting the left and right ear canals being located at approximately 0.00 mm. See Fig. 1 for abbreviations.

how their respective anatomical sites are located on the face. The stimulation sites extending in an anterior–posterior direction along the lower jaw and chin were transposed into ECD locations extending in a posterior–anterior direction along the sagittal MRI. On the same sagittal section, the ECD locations corresponding to corner of the mouth and midzygomatic sites appeared inferior relative to the ECD locations for sites along the lower jaw: mandibular angle, ½ mandible–chin, and ¾ mandible–chin.

Similarly, a detailed map of the hand showed good spatial resolution of closely spaced anatomical sites. On a coronal section, the ECD locations which corresponded to the anterior fingertips of left digits 3, 4, and 5 appeared diagonally stacked in a radially pointing column parallel to another similarly oriented column consisting of the ECD locations which corresponded to the left anterior palmar pads for digits

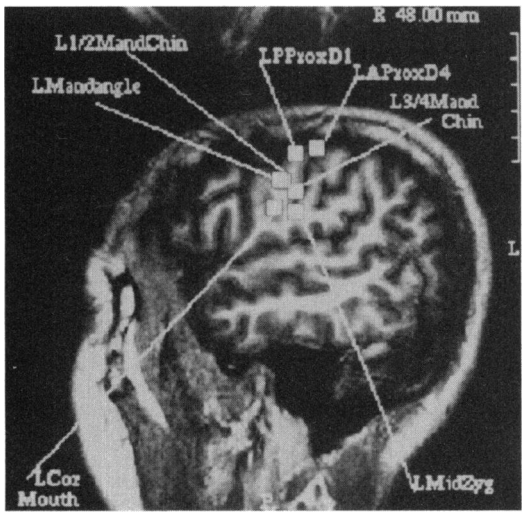

FIG. 3. Sagittal section on subject 1 showing location of dipoles corresponding to tactile sites on the left face and digits. See Fig. 1 for abbreviations.

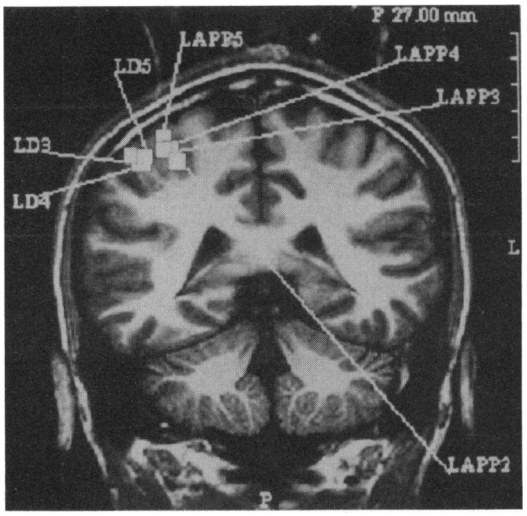

FIG. 4. Coronal section on subject 1 showing location of dipoles corresponding to tactile sites on the left anterior digits and palmar pads. See Fig. 1 for abbreviations.

2, 3, 4, and 5. The ECD locations which corresponded to these palmar pads seemed to be arranged in an orderly fashion with palmar pad 2 being located the deepest, and palmar pads 3, 4, and 5 being located in progressively more superficial locations (Fig. 4). On this coronal slice, the palmar pads were located in a separate cortical area medial to the fingertips. The anterior and posterior side of the fingertips may also be distinguished. In a coronal section, the anterior side of the first and second digits stacked into a radially pointing column, whereas the ECD location corresponding to the posterior side of the first digit appeared to lie in a separate cortical area. The anterior and posterior sides of digit one seemed to lie in two different sulci on opposite sides of the same gyrus (Fig. 5).

The forearm, upper arm, and anterior and posterior sides of the wrist were similarly separable from one another on the MRI overlays. On the coronal section, the ECD locations corresponding to the anterior and posterior sides of the right wrist along with several ECD locations corresponding to sites on the right forearm appeared to lie along the same radial line (Fig. 6). The ECD location for the anterior wrist was deep within the sulcus, while the ECD for the posterior side of the

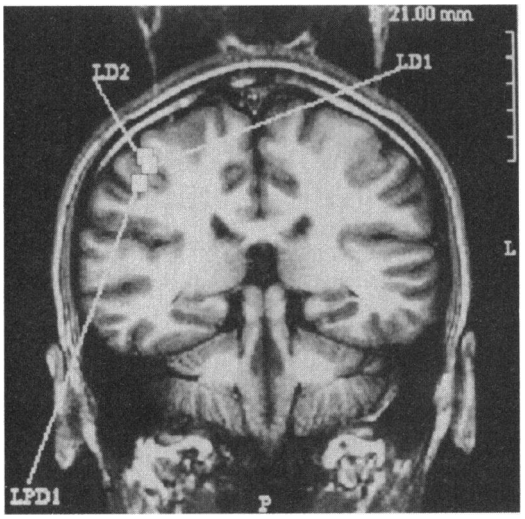

FIG. 5. Coronal section on subject 1 showing location of dipoles corresponding to tactile sites on the anterior and posterior sides of left digit 1. LPD1, left posterior digit 1. See Fig. 1 for abbreviations.

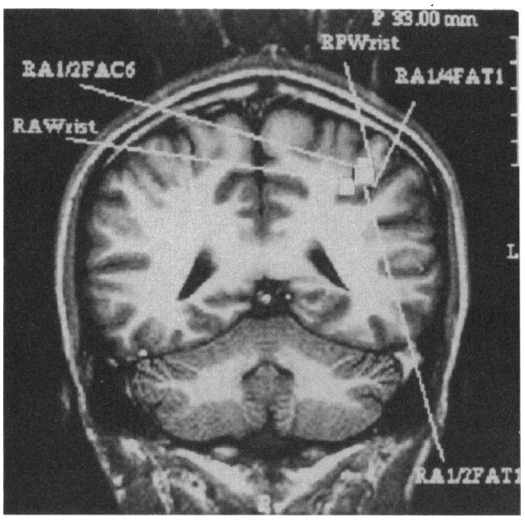

FIG. 6. Coronal section on subject 1 showing location of dipoles corresponding to tactile sites on the right forearm. See Fig. 1 for abbreviations.

same wrist was more superficial and lateral to the anterior wrist (Fig. 6).

Sagittal and coronal sections consistently showed the ECD locations corresponding to sites on the hand being in a region superior to the ECD locations corresponding to sites on the face (Figs. 3 and 7). The ECD locations representing tactile sites along the lower jaw extending from the mandibular angle to ¾ mandible–chin appeared to lie closest to the ECD locations representing tactile sites on the hand (Fig. 3). The ECD locations representing the corner of mouth and midzygomatic sites appeared inferior to the ECD locations representing the tactile sites along the lower jaw and chin (Fig. 3).

DISCUSSION

This study demonstrates that MEG recordings modeled as a single ECD can map the primary somatosensory region with high spatial resolution and that the number of distinguishable somatosensory sites is substantially greater than has been previously reported for humans (6, 10–18). Closely spaced tactile sites on the skin surface can map to distinguishable separate cortical areas on the MRI overlays by using a single ECD model. Similar results were obtained in five additional subjects, normal females. Results of right-left symmetries will be reported separately. The fingertips were distinguishable from their respective palmar pads on the anterior side of the hand (Fig. 4). The anterior and posterior sides of the left first digit and right wrist were also discernible (Figs. 5 and 6). Similarly, closely spaced facial tactile spots such as the upper lip, corner of mouth, and mental protuberance separated out well (Fig. 2).

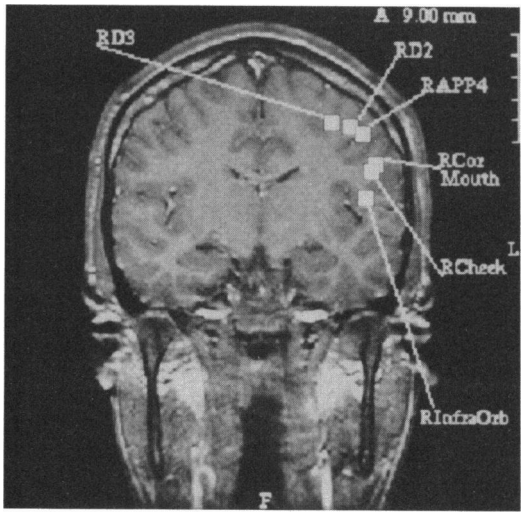

FIG. 7. Coronal section on subject 2 showing dipoles corresponding to tactile sites on the right face, hand, and digits. See Fig. 1 for abbreviations.

The ECD locations which represented light pressure sensation for the tactile sites along the lower jaw and chin appeared to lie in a group which was separate from the rest of the face, and which was closer to the ECD locations which represented light tactile sensation in the digits (Fig. 3). The superior positioning of the ECD locations representing the fingers relative to the ECD locations representing the face agreed with Penfield's observations (1). The ECD location representing sensation for the upper lip was, as Penfield also observed, adjacent to the face region (Fig. 2). It appeared to be slightly superior and lateral to the ECD location for the mental protuberance and corner of the mouth. However, the closer proximity of the lower jaw and chin to the fingers as compared to the rest of the face was not observed by Penfield. Penfield's map of the somatosensory system showed the superior parts of the face being located closer to the fingers and hand than the more inferior facial areas. When taken with recent observations by Ramachandran *et al.* (22, 23) regarding perceptual correlates of massive cortical reorganization in adult humans, and by Pons *et al.* (24) concerning massive cortical reorganization after sensory deafferentation in adult monkeys, our data support the theory that the lower facial areas are located closer to the fingers as compared to the upper facial regions.

The ECD locations which represented light pressure sensation on the digits were in a region slightly inferior and lateral to the ECD locations representing similar sensation in the palmar pads of the hand for subject 1 (Fig. 4). This observation agreed with Penfield's general findings. However, in subject 2 it appeared that the ECD locations for the digits were slightly superior and medial to the ECD location for the palmar pad (Fig. 7). In these two unrelated subjects there appeared to be some intersubject variability in the organization of the somatosensory system. A study done on monozygotic twins revealed a greater similarity in the size and shape of the corpus collosum in twin pairs than in randomly paired, unrelated control subjects (25). Thus it would be interesting to see whether genetics plays a similar role in the organization of the somatosensory system.

In agreement with Penfield (1), the ECD location which represented sensation on the anterior wrist was adjacent to and slightly inferior to the ECD locations which represented sensation on the anterior forearm (Fig. 6). However, the ECD location for the posterior wrist was superior and lateral to the ECD locations for the anterior forearm and anterior wrist. In addition, the ECD locations for the anterior and posterior sides of the first digit appeared to map to separate distinct cortical locations (Fig. 5) which Penfield did not distinguish between in his findings.

The ability to map the somatosensory system noninvasively with high spatial resolution will allow the examination of questions in humans which so far have been addressed only invasively in experimental animals. Questions regarding the organization and variability of the somatosensory cortex and the nature of adult neural plasticity may now all be examined in humans by using MEG (26–29).

The authors thank Eugene Hirschkoff for his comments. This work was funded in part by the National Institute for Mental Health, the Armstrong MacDonald Foundation, Biomagnetic Technologies,

Inc., and the McDonnell–Pew Center for Cognitive Neuroscience. This is paper NP7753 from The Scripps Research Institute.

1. Penfield, W. & Rasmussen, T. (1950) *The Cerebral Cortex of Man* (Macmillan, New York), p. 248.
2. Woolsey, C. N., Erickson, T. C. & Gilson, W. E. (1979) *J. Neurosurg.* **51,** 476–506.
3. Baumgartner, C., Barth, D. D., Levesque, M. F. & Sutherling, W. W. (1991) *Electroencephalogr. Clin. Neurophysiol.* **78,** 56–65.
4. Wood, C. C., Spencer, D. D., Allison, T., McCarthy, G., Williamson, P. D. & Goff, W. R. (1988) *J. Neurosurg.* **68,** 99–111.
5. Allison, T. (1987) *Yale J. Biol. Med.* **60,** 143–150.
6. Fox, P. T., Burton, H. & Raichle, M. E. (1987) *J. Neurosurg.* **67,** 34–43.
7. Luders, H., Dinner, D. S., Lesser, R. P. & Morris, H. H. (1986) *J. Clin. Neurophysiol.* **3,** 75–84.
8. Hamalainen, H., Kekoni, J., Sams, M., Reinikainen, K. & Naatanen, R. (1990) *Electroencephalogr. Clin. Neurophysiol.* **75,** 13–21.
9. Duff, T. A. (1980) *Electroencephalogr. Clin. Neurophysiol.* **49,** 452–460.
10. Baumgartner, C., Doppelbauer, A., Sutherling, W. W., Zeitlhofer, J., Lindinger, G., Lind, C. & Deecke, L. (1991) *Neurosci. Lett.* **134,** 103–108.
11. Sutherling, W. W., Crandall, P. H., Darcey, T. M., Becker, D. P., Levesque, M. F. & Barth, D. S. (1988) *Neurology* **38,** 1705–1714.
12. Hari, R. (1991) *J. Clin. Neurophysiol.* **8,** 157–169.
13. Suk, J., Ribary, U., Cappell, J., Yamamoto, T. & Llinas, R. (1991) *Electroencephalogr. Clin. Neurophysiol.* **78,** 185–196.
14. Brenner, D., Lipton, J., Kaufman, L. & Williamson, S. J. (1978) *Science* **199,** 81–83.
15. Wood, C. C., Cohen, D., Cuffin, B. N., Yarita, M. & Allison, T. (1985) *Science* **227,** 1051–1053.
16. Okada, Y. C. (1984) *Exp. Brain Res.* **56,** 197–205.
17. Kaukoranta, E., Hamalainen, M., Sarvas, J. & Hari, R. (1986) *Exp. Brain Res.* **63,** 60–66.
18. Huttunen, J. (1986) *Eur. J. Physiol.* **407,** 129–133.
19. Williamson, S. J. & Kaufman, L. (1987) in *Handbook of Electroencephalography and Clinical Neurophysiology*, eds. Gevins, A. & Remond, A. (Elsevier, Amsterdam), Vol. 1, pp. 405–447.
20. Pantev, C., Gallen, C., Hampson, S., Buchanan, S. & Sobel, D. (1991) *Am. J. Electroencephalogr. Technol.* **31,** 83–101.
21. Gallen, C. C., Schwartz, B. J., Rieke, K., Pantev, C., Sobel, D., Hirschkoff, E. & Bloom, F. E. (1993) *Electroencephalogr. Clin. Neurophysiol.*, in press.
22. Ramachandran, V. S., Stewart, M. & Rogers-Ramachandran, D. C. (1992) *NeuroReport* **3,** 583–586.
23. Ramachandran, V. S., Rogers-Ramachandran, D. & Stewart, M. (1992) *Science* **258,** 1159–1160.
24. Pons, T. P., Garraghty, P. E., Ommaya, A. K., Kaas, J. H., Taub, E. & Mishkin, M. (1991) *Science* **252,** 1857–1860.
25. Oppenheim, J. S., Skerry, J. E., Tramo, M. J. & Gazzaniga, M. S. (1989) *Ann. Neurol.* **26,** 100–104.
26. Mogilner, A., Grossman, J. A. I., Ribary, U., Lado, F., Volkmann, J., Joliot, M. & Llinas, R. R. (1992) *Soc. Neurosci.* **1,** 316.11.
27. Merzenich, M. M., Kaas, J. H., Wall, J. T., Nelson, R. J., Sur, M. & Felleman, D. J. (1983) *Neuroscience (Oxford)* **8,** 33–55.
28. Merzenich, M. M., Kaas, J. H., Wall, J. T., Sur, M., Nelson, R. J. & Felleman, D. J. (1983) *Neurosciences (Cambridge Mass)* **10,** 639–665.
29. Merzenich, M. M., Nelson, R. J., Stryker, M. P., Cynader, M. S., Schoppmann, A. & Zook, J. M. (1984) *J. Comp. Neurol.* **224,** 591–605.